CHAPTER 141

FINITE ELEMENT MODEL OF TWO LAYER COASTAL CIRCULATION

by

JOHN D. WANG [1]

JEROME J. CONNOR [2]

ABSTRACT

A set of "averaged" partial differential equations for the circulation in a two layered coastal water is established by assuming each layer to be vertically homogeneous and by performing a vertical integration over the layer thicknesses. Since the phenomena to be investigated typically consist of long waves such as a tidal wave, the hydrostatic pressure assumption is also introduced. The finite element method is employed to transform the partial differential equations to a discrete system of ordinary differential equations which are solved using an implicit time stepping method similar to the trapezoidal rule, but with the variables (elevation and flows) staggered in time. A linear stability analysis shows the initial value problem to be unconditionally stable. In practice, instability due to boundary conditions and non-linearity sets in.

Comparisons between computed and analytical solutions for simple cases give good agreement. The tidal excitation of Massachusetts Bay, represented as a rectangular basin with opening on one side is presented as an illustrative example.

INTRODUCTION

The rapidly increasing development of our coastal areas has generated the need for a better understanding of the physical processes in a coastal water body and for methods to predict the effect of man-made changes. In particular, significant effort has been directed at determining flow patterns and mass transport [1, 7, 8, 10, 13]. For complex phenomena such as these, one usually has to resort to physical or numerical models to obtain solutions. This paper describes a numerical technique, based on the finite element method, to predict tide and wind driven circulation for a stable stratified water body in which two distinct layers can be distinguished, a condition often found in coastal waters during summer time. Due to the

---

1) Graduate Student, R.M. Parsons Laboratory for Water Resources and Hydrodynamics, M.I.T., Cambridge, Massachusetts, U.S.A.

2) Professor of Civil Engineering, R.M. Parsons Laboratory for Water Resources and Hydrodynamics, M.I.T., Cambridge, Massachusetts, U.S.A.

increased solar radiation a warmer, lighter surface layer forms with a rather abrupt density change between layers. It is reasonable to approximate the problem as consisting of two vertically homogeneous layers, thereby reducing the degree of complexity.

Until recently, numerical models of coastal circulation have been almost exclusively of the finite difference type. In previous works by the authors [4] a rigorous formulation and solution strategy for 2-dimensional one layer flow using the finite element method has been presented. This method is particularly attractive with respect to formulation and specifying boundary conditions. However, the error and stability aspects for hyperbolic and elliptic boundary value problems treated with finite element methods are not completely resolved. A stability analysis of the linearized system is presented here for some simple schemes. Apart from numerical problems, there are unresolved questions concerning the actual physical processes such as momentum and mass transfer between layers and at open boundaries. These are areas where much more research is needed before truly predictive capabilities are at hand.

MATHEMATICAL FORMULATION

The two layer flow problem is governed by the conservation of mass and momentum requirements. For illustration, it is useful to look at the one layer case first. Assuming that the water column is fairly well mixed it is reasonable to simplify the problem by performing a vertical integration using Leibnitz's rule and the boundary conditions on the surface and bottom. Fig. 1 shows a definition sketch with a horizontal x-y coordinate system, z vertically upwards, surface elevation η and bottom at z=-h. The dependent variables are the total water depth H (or alternatively η) and the total volume flows per unit width in x and y directions.

$$H = h + \eta \tag{1}$$

$$q_x = \int_{-h}^{\eta} u dz \qquad q_y = \int_{-h}^{\eta} v dz \tag{2}$$

The form of the governing equations have been shown to be [4]:

$$\frac{\partial}{\partial t}(\rho H) + \frac{\partial}{\partial x}q_x + \frac{\partial}{\partial y}q_y = q_I \tag{3}$$

$$\frac{\partial}{\partial t}q_x + \frac{\partial}{\partial x}(\bar{u}q_x) + \frac{\partial}{\partial y}(\bar{u}q_y) = fq_y + B_x + \frac{\partial}{\partial x}(F_{xx} - F_p) + \frac{\partial}{\partial y}F_{yx}$$

$$\frac{\partial}{\partial t}q_y + \frac{\partial}{\partial x}(\bar{v}q_x) + \frac{\partial}{\partial y}(\bar{v}q_y) = - fq_x + B_y + \frac{\partial}{\partial x} F_{xy} + \frac{\partial}{\partial y}(F_{yy} - F_p) \tag{4}$$

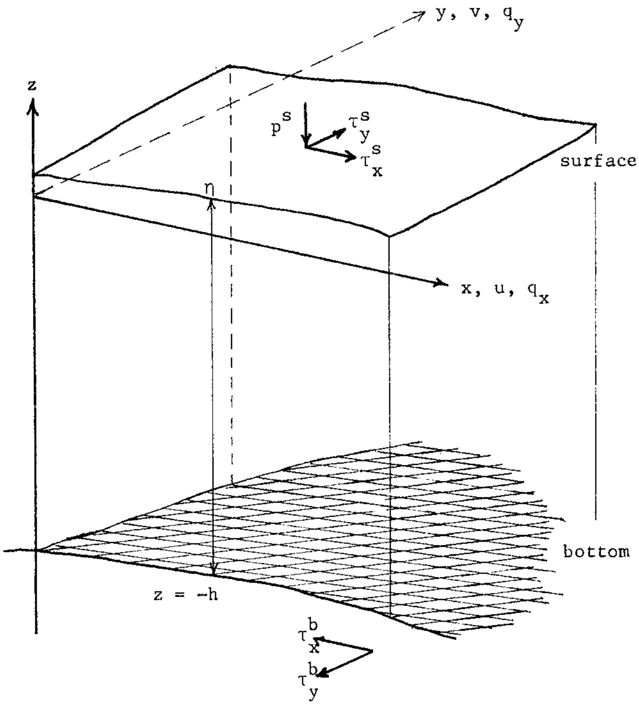

Fig. 1. Definition sketch for one layer flow.

here

$$F_p = \frac{1}{\rho_o} \int_{-h}^{\eta} p dz - \frac{1}{2} gh^2$$

$$= g(h\eta + \frac{1}{2}\eta^2) + \frac{1}{2} \frac{\Delta\rho}{\rho_o} gH^2 + \frac{p^s}{\rho_o} H \tag{5}$$

$$B_{x_i} = \frac{1}{\rho_o}(p^s \frac{\partial H}{\partial x_i} + \Delta\rho g H \frac{\partial h}{\partial x_i} + \rho_o g y \frac{\partial h}{\partial x_i} + \tau_{x_i}^s - \tau_{x_i}^b); \; i = 1,2 \tag{6}$$

and q_I denotes an internal source, $f = 2\Omega\sin\phi$ is the Coriolis parameter, (F_{xx}, F_{xy}, F_{yy}) are internal stresses; $\bar{u}$ and $\bar{v}$ are average velocities; F_p is the excess integrated pressure, p^s is the barometric pressure on the surface; and τ^s, τ^b are surface and bottom shear stresses. For convenience we frequently write x_1, x_2 for x, y. The mass density $\rho = \rho_o + \Delta\rho$ is replaced by the constant mean value ρ_o everywhere except in the hydrostatic pressure (5). This is known as the Boussinesque approximation.

The internal stress terms F_{xx}, F_{xy}, F_{yy} represent the specific momentum transfers due to viscosity, turbulence and vertical shear. Their general form is:

$$F_{x_i x_j} = \int_{-h}^{\eta} \left\{ \tau^{\nu}_{x_i x_j}/\rho_o - <(u_i' u_j') + (u_i'' \cdot u_j'')>\text{ensemble} - u_i'' u_j'' \right\} dz \qquad i,j = 1, 2 \tag{7}$$

where τ^{ν} is the molecular stress term; u' is the turbulent fluctuation of the velocity, u'' is the velocity deviation from the vertical mean value $\bar{u}$, and u''' is the deviation of the turbulent fluctuation. As indicated in (7) all turbulent fluctuations are ensemble averaged.

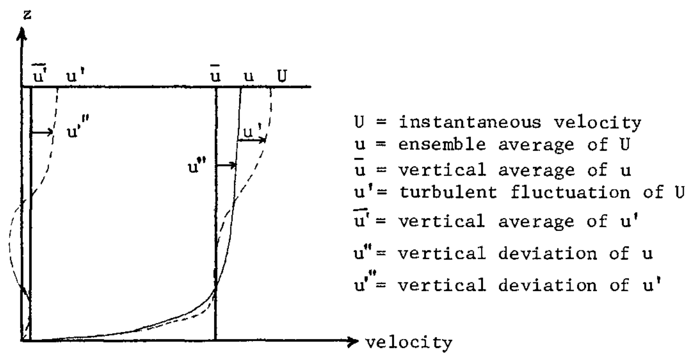

Fig. 2. Velocity distribution in the vertical and its components.

One of the most significant difficulties with an averaged or integrated formulation is the occurrence of additional variables due to the non-linear terms. In turbulence theory, these variables give rise to the so-called Reynolds stresses and the phenomenon is often called the closure problem because there are more variables than equations. For our approach, we have lumped all these apparent stresses together with viscous stresses in the internal specific force measures (force per unit width and density) F_{xx}, F_{xy}, F_{yy}. An engineering solution has been to interpret the apparent stresses as momentum transfer and represent them by a diffusion process analogous to Newton's law for viscous shear. Following this approach, we express the force measures as

$$F_{x_i x_j} = E_{ij}\left(\frac{\partial q_j}{\partial x_i} + \frac{\partial q_i}{\partial x_j}\right) \qquad \text{no summing over } i,\ j \tag{8}$$

Once the "eddy diffusion" coefficient matrix E_{ij} is specified, the problem is closed. However, contrary to molecular viscosity which is a fluid property, the E_{ij}'s are functions of the flow field. More specifically they can depend on the flow, shear stresses on bottom and surface, depth and time. By definition $F_{ij} = F_{ji}$ and therefore E_{ij} must be symmetric. If E_{ij} is taken as anisotropic, the principal directions should usually be defined along and perpendicular to the local velocity direction. The effect of the internal stresses is to dissipate or generate energy depending on whether E_{ij} is positive or negative [5,11]. At present little is known about the validity of (8), in particular what is the relationship for E_{ij} in terms of flow parameters. It will be shown later that positive eddy viscosity improves numerical stability, mainly by dissipating high frequency energy.

The equations governing vertically integrated layered flow follow by generalizing (3), (4) and are written as

$$\frac{\partial H_k}{\partial t} + \frac{\partial}{\partial x} q_{xk} + \frac{\partial}{\partial y} q_{yk} = q_k \tag{9}$$

$$\frac{\partial q_{xk}}{\partial t} + \frac{\partial}{\partial x}(\bar{u}_k q_{xk}) + \frac{\partial}{\partial y}(\bar{u}_k q_{yk})$$

$$= f q_{yk} + \frac{\partial}{\partial x}(F_{xxk} - F_{pk}) + \frac{\partial}{\partial y} F_{yxk} + \frac{1}{\rho_k}\left\{\tau_{xk} - \tau_{xk-1} + p_k \frac{\partial \eta_k}{\partial x} - p_{k-1} \frac{\partial \eta_{k-1}}{\partial x}\right\} \tag{10}$$

$$\frac{\partial q_{yk}}{\partial t} + \frac{\partial}{\partial x}(\bar{v}_k q_{xk}) + \frac{\partial}{\partial y}(\bar{v}_k q_{yk})$$

$$= -fq_{xk} + \frac{\partial}{\partial x}F_{xyk} + \frac{\partial}{\partial y}(F_{yyk} - F_{pk}) + \frac{1}{\rho_k}\left\{\tau_{yk} - \tau_{yk-1} + p_k\frac{\partial \eta_k}{\partial y} - p_{k-1}\frac{\partial \eta_{k-1}}{\partial y}\right\}$$

where the notation for layer k is defined in Figure (3).

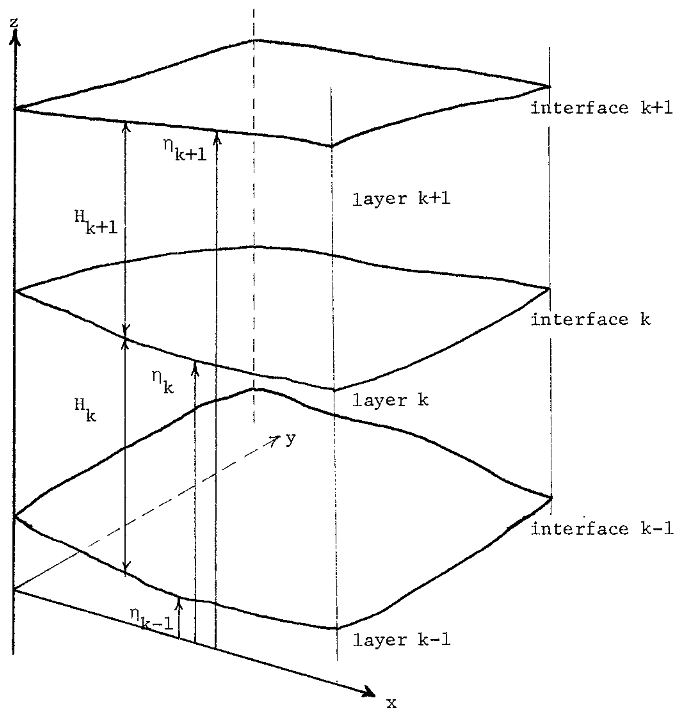

Fig. 3. Definition sketch for multilayered flow.

We still assume hydrostatic pressure, i.e., the pressure at the k'th interface is given by $p_{k-1} - p_k = \rho_k g H_k$ (11)

For two-layer flow, p_2 = atmospheric pressure

The equilibrium equations on the boundary take the following forms:

$$F_{nnk} = F^*_{nnk} \quad \text{on } S_k \tag{12}$$

where F^*_{nnk} is the prescribed specific force measure normal to the boundary on layer k, S_k.

Conservation of mass (continuity) is satisfied when

$$q_{nk} = q^*_{nk} \text{ on } S_k \tag{13}$$

Here q^*_{nk} is the prescribed normal boundary flux for layer k. When the eddy viscosity terms are retained in the formulation, additional equilibrium conditions on tangential forces

$$F_{nsk} = F^*_{nsk} \tag{14}$$

and flows

$$q_s = q^*_s \tag{15}$$

can be specified.

The interfacial shear stresses are evaluated with the most commonly used relation:

$$\begin{Bmatrix} \tau_{xk} \\ \tau_{yk} \end{Bmatrix} = \begin{Bmatrix} \bar{u}_k - \bar{u}_{k-1} \\ \bar{v}_k - \bar{v}_{k-1} \end{Bmatrix} \rho_k C_{fk} [(\bar{u}_k - \bar{u}_{k-1})^2 + (\bar{v}_k - \bar{v}_{k-1})^2]^{\frac{1}{2}} \tag{16}$$

Investigations have shown the dimensionless friction factor, C_{fk}, to be dependent on at least Reynolds number and densimetric Froude number (Richardson number) [2].

Summarizing the formulation, the dependent variables are the volume flows per unit width in each layer, q_{xk}, q_{yk} and the layer thicknesses H_k. The governing equations are given by (9) - (10) which apply in the interior and (12) - (13) on the boundaries.

THE WEAK FORM

There has been considerable recent effort by mathematicians directed at proving that the solutions obtained from the flow equations, notably the Navier Stokes equations, are unique [6]. In one approach, the differential equations are transformed to an integral expression which is called the weak or Galerkin form [9, 12]. When the weak form has a unique solution, this will also be the unique solution of the original equations, and the weak form is then called the generalized form. Thus, the mathematical problem reduces to showing that the weak form has a unique solution. There are indications [6, 12] that the generalized equations constitute the well-posed form of the problem In what follows, we cast the problem into its weak form and use this as the basis for the finite element approximation. No attempt is made here to present a mathematical proof of uniqueness. However, we do present comparisons with analytical solutions.

The weak form is derived by weighting the continuity and equilibrium equations, and integrating over the total area.

$$\iint_{A_k} \left\{ \frac{\partial H}{\partial t} + \frac{\partial q_x}{\partial x} + \frac{\partial q_y}{\partial y} - q \right\}_k \cdot \Delta H_k dA + \int_{S_k} \left\{ q_n - q_n^* \right\}_k \cdot \Delta H_k ds = 0 \tag{17}$$

$$\begin{aligned}\iint_{A_k} \Big[& \left\{ \frac{\partial q_x}{\partial t} + \frac{\partial}{\partial x}(\bar{u} q_x) + \frac{\partial}{\partial y}(\bar{u} q_y) - f q_y \right. \\ & \left. + \frac{\partial}{\partial x}(F_p - F_{xx}) - \frac{\partial}{\partial y} F_{yx} - \tau_x - p\frac{\partial \eta}{\partial x} \right\}_k \\ & + \left\{ \tau_x + p\frac{\partial \eta}{\partial x} \right\}_{k-1} \Big] \Delta q_{xk} dA \\ & + \int_{S_k} \left\{ F_{nx} - F_{nk}^* \right\}_k \Delta q_{xk} \, ds = 0 \end{aligned} \tag{18}$$

$$\begin{aligned}\iint_{A_k} \Big[& \left\{ \frac{\partial q_y}{\partial t} + \frac{\partial}{\partial x}(\bar{v} q_x) + \frac{\partial}{\partial y}(\bar{v} q_y) + f q_x - \frac{\partial}{\partial x} F_{xy} \right. \\ & \left. + \frac{\partial}{\partial y}(F_p - F_{yy}) - \tau_y - p\frac{\partial \eta}{\partial y} \right\}_k \end{aligned}$$

$$+ \left\{\tau_y + p\frac{\partial \eta}{\partial y}\right\}_{k-1}] \, \Delta q_{yk} \, dA$$

$$+ \int_{S_k} \left\{F_{ny} - F^*_{ny}\right\}_k \Delta q_{yk} \, ds = 0$$

where ΔH, Δq_x, Δq_y are arbitrary finite continuous functions and F^*_{nx}, F^*_{ny} are the prescribed values of the x and y components of the normal specific force measure. Applying Gauss's theorem for partial integration to the momentum equations yields the desired form:

$$\iint_{A_k} [(\left\{\frac{\partial q_x}{\partial t} + \frac{\partial}{\partial x}(\bar{u} q_x) + \frac{\partial}{\partial y}(\bar{u} q_y) - f q_y - \tau_x - p\frac{\partial \eta}{\partial x}\right\}_k$$

$$+ \left\{\tau_x + p\frac{\partial \eta}{\partial x}\right\}_{k-1}) \, \Delta q_{xk} + \left\{(F_{xx} - F_p) \frac{\partial \Delta q_x}{\partial x}\right.$$

$$\left. + F_{yx} \frac{\partial \Delta q_x}{\partial y}\right\}_k] \, dA$$

$$- \int_{S_k} \left\{F^*_{nx} \Delta q_x\right\}_k ds = 0 \tag{19}$$

$$\iint_{A} [(\left\{\frac{\partial q_y}{\partial t} + \frac{\partial}{\partial x}(\bar{v} q_x) + \frac{\partial}{\partial y}(\bar{v} q_y) + f q_x - \tau_y - p\frac{\partial \eta}{\partial y}\right\}_k$$

$$+ \left\{\tau_y + p\frac{\partial \eta}{\partial y}\right\}_{k-1}) \, \Delta q_{yk} + \left\{F_{xy} \frac{\partial \Delta q_y}{\partial x}\right.$$

$$\left. + (F_{yy} - F_p) \frac{\partial \Delta q_y}{\partial y}\right\}_k] \, dA$$

$$- \int_{s} \left\{F^*_{ny} \Delta q_y\right\}_k ds = 0$$

FINITE ELEMENT DISCRETIZATION

The discretization in space is obtained by applying the finite element technique, which allows for a flexible grid configuration, easy handling of complex boundaries and topography, and straightforward mathematical representation.

A boundary segment is classified according to the boundary condition for the segment. On S_o, the open ocean boundary, the layer depths are prescribed. On S_q, which can be either a land boundary or across a stream, the normal flux is prescribed.

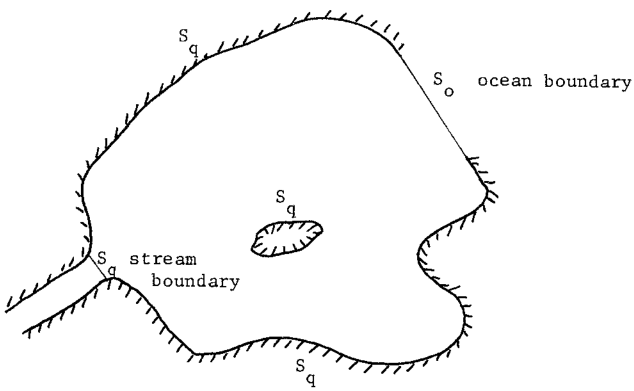

Fig. 4. Boundary classification.

When eddy viscosity is included, lateral shear can exist and the tangential forces and fluxes on the boundaries must also be matched. Prescribing the tangential flow, usually as a no-slip condition, does not cause any conceptual problems. However, the need to know both normal and tangential forces presents a serious data acquisition problem since layer depths can no longer be used as a replacement for the pressure force.

The weak form is the natural basis for the finite element method. We require the weighting functions ΔH, Δq_x, Δq_y to be admissible, that is, described by the same shape functions as the dependent variables and satisfying the homogeneous boundary conditions. With these restrictions, ΔH, Δq_x, Δq_y can be interpreted as admissible variations of H, q_x, q_y.

The integrals

$$\int_{S_k} \left\{ q_n - q_n^* \right\}_k \Delta H_k ds \ , \tag{a}$$

$$\int_{Sq_k} \left\{ -F_{nx}^* \right\}_k \Delta q_{xk} ds \ ,$$

$$\int_{Sq_k} \left\{ -F_{ny}^* \right\}_k \Delta q_{yk} ds \tag{b}$$

vanish and we are left with

$$\iint_{A_k} \left\{ \frac{\partial H}{\partial t} + \frac{\partial q_x}{\partial x} + \frac{\partial q_y}{\partial y} - q \right\}_k \Delta H_k dA = 0 \tag{20}$$

$$\iint_{A_k} [(\left\{ \frac{\partial q_x}{\partial t} + \frac{\partial}{\partial x}(\bar{u} q_x) + \frac{\partial}{\partial y}(\bar{u} q_y) - f q_y - \tau_x - p\frac{\partial \eta}{\partial x} \right\}_k$$

$$+ \left\{ \tau_x + p\frac{\partial \eta}{\partial x} \right\}_{k-1}) \ \Delta q_{xk} + \left\{ (F_{xx} - F_p) \frac{\partial \Delta q_x}{\partial x} \right.$$

$$\left. + F_{yx} \frac{\partial \Delta q_x}{\partial y} \right\}_k] \ dA$$

$$- \int_{S_{ok}} \left\{ F_{nx}^* \ \Delta q_x \right\}_k ds = 0$$

$$\iint_{A_k} [(\left\{ \frac{\partial q_y}{\partial t} + \frac{\partial}{\partial x}(\bar{v} q_x) + \frac{\partial}{\partial y}(\bar{v} q_y) + f q_x - \tau_y - p\frac{\partial \eta}{\partial y} \right\}_k \tag{21}$$

$$+ \left\{ \tau_y + p\frac{\partial \eta}{\partial y} \right\}_{k-1}) \ \Delta q_y + \left\{ F_{yx} \frac{\partial \Delta q_y}{\partial x} \right.$$

$$+ (F_{yy} - F_p) \frac{\partial \Delta q_y}{\partial y} \Big\}_k] dA$$

$$- \int_{S_{ok}} \Big\{ F^*_{\eta y} \; \Delta q_y \Big\}_k ds = 0$$

We have found that, under normal circumstances, the force integrals (b) on the prescribed flow boundary which, in theory, vanish have to be retained as a correction in practical application. This is due to the fact that the normal direction chosen for a boundary node point is the average direction for the adjacent segments, and specifying q_n=0 for the node does not (unless the sides are parallel) result in q_n=0 for the segments. This correction tends to zero as the grid is refined; but for practical grid sizes, (20) and (19) should be used.

All variables are now expressed in terms of the element nodal values and functions defining the spatial variation over the element domain,

$$f = \phi_i \quad F_i \tag{22}$$

F_i are the nodal values and ϕ_i are prescribed functions of x and y.

Substituting (22) in (19) - (20) results in a system of ordinary differential equations relating the nodal variables

$$M_H \dot{H} + DQ = P_H \tag{23}$$

$$M_Q \dot{Q} - D^T H + CQ + EQ = P_Q \tag{24}$$

where H is a vector containing the nodal values of layer thickness, Q contains the nodal fluxes listed as $[q_{x_1} \; q_{y_1} \cdots q_{x_i} \; q_{x_i} \cdots q_{x_n} \; q_{y_n}]$ with i being the node number; the dot denotes time differentiation, P_H and P_Q are vectors containing non-linear and forcing terms. Although the elements of the coefficient matrices depend on grid and element type, they do have certain invariant properties: M and E (eddy viscosity) are symmetric and positive definite, and C (Coriolis) is skewsymmetric.

TIME INTEGRATION

Integration of (23) - (24) through time is carried out with the trapezoidal rule, a simple implicit scheme. The assumption is made that non-linear, Coriolis, and eddy viscosity terms are of relatively minor importance, hence a simple backward difference approximation is used for them. Our starting point is

$$\underset{\sim}{M}_H \dot{\underset{\sim}{H}} + \underset{\sim}{D}\underset{\sim}{Q} = \underset{\sim}{P}_H \tag{25}$$

$$\underset{\sim}{M}_Q \dot{\underset{\sim}{Q}} - \underset{\sim}{D}^T \underset{\sim}{H} = \underset{\sim}{P}_Q - \underset{\sim}{C}\,\underset{\sim}{Q} - \underset{\sim}{E}\underset{\sim}{Q} \tag{26}$$

A direct application of the trapezoidal rule is possible. However, storage requirements are excessive since one has to solve for all 3N (N is number of nodes) unknowns at the same time, and furthermore the coefficient matrix is unsymmetric. 18N·BW words of storage are required where BW is the minimum bandwidth.

To circumvent the storage problem a split-time scheme was devised. The variables H and Q are staggered in time such that H is defined at time t, t + Δt, and Q is defined at t - $\frac{1}{2}\Delta$t, t + $\frac{1}{2}\Delta$t etc. In this way, we can write (25) as

$$\underset{\sim}{M}_H \dot{\underset{\sim}{H}} = \underset{\sim}{P}_H - \underset{\sim}{D}\underset{\sim}{Q} \tag{27}$$

$$\underset{\sim}{M}_Q \dot{\underset{\sim}{Q}} = \underset{\sim}{P}_Q - \underset{\sim}{C}\underset{\sim}{Q} - \underset{\sim}{E}\underset{\sim}{Q} + \underset{\sim}{D}^T \underset{\sim}{H} \tag{28}$$

and solve (27) and (28) in successive order. The coefficient matrices remain symmetric, and required storage is reduced to 5N·BW words. In addition the accuracy is improved because the difference approximations are central rather than backward, and also significant economy in computation time is realized.

The stability of the linearised, homogeneous initial value problems can be investigated with the matrix method. We define

$$\underset{\sim}{M}_1 = \underset{\sim}{M}_Q + \theta\Delta t\ \underset{\sim}{E} \tag{29}$$

$$\underset{\sim}{M}_2 = \underset{\sim}{M}_Q - (1-\theta)\Delta t\underset{\sim}{E} \tag{30}$$

and write (27) - (28) as:

$$(\underset{\sim}{M}_1 + \theta\Delta t\underset{\sim}{C})\underset{\sim}{Q}_{n+\frac{1}{2}} = (\underset{\sim}{M}_2 - (1-\theta)\Delta t\underset{\sim}{C})\underset{\sim}{Q}_{n-\frac{1}{2}} + \Delta t\underset{\sim}{D}^T\underset{\sim}{H}_n + \Delta t\ \underset{\sim}{P}_H \tag{31}$$

$$\underset{\sim}{M}_H\underset{\sim}{H}_{n+1} = -\Delta t\underset{\sim}{D}\underset{\sim}{Q}_{n+\frac{1}{2}} + \underset{\sim}{M}_H\underset{\sim}{H}_n + \Delta t\ \underset{\sim}{P}_H \tag{32}$$

Their combined form is

$$\begin{Bmatrix} \underset{\sim}{M}_1 + \theta\Delta t\underset{\sim}{C} & \underset{\sim}{0} \\ \Delta t\underset{\sim}{D} & \underset{\sim}{M}_H \end{Bmatrix} \begin{Bmatrix} \underset{\sim}{Q}_{n+\frac{1}{2}} \\ \underset{\sim}{H}_{n+1} \end{Bmatrix} = \begin{Bmatrix} \underset{\sim}{M}_2 - (1-\theta)\Delta t\underset{\sim}{C} & \Delta t\underset{\sim}{D}^T \\ \underset{\sim}{0} & \underset{\sim}{M}_H \end{Bmatrix} \begin{Bmatrix} \underset{\sim}{Q}_{n-\frac{1}{2}} \\ \underset{\sim}{H}_n \end{Bmatrix} + \Delta t \begin{Bmatrix} \underset{\sim}{P}_Q \\ \underset{\sim}{P}_H \end{Bmatrix} \tag{33}$$

Taking θ equal to 1 corresponds to a fully implicit treatment of Coriolis and eddy viscosity, and θ equal to 0 is equivalent to a completely explicit treatment. Values between 0 and 1 are also possible. We use $\theta = 0$ in our "split-time" scheme.

By defining

$$\underset{\sim}{X}_{n+1} = \begin{Bmatrix} \underset{\sim}{Q}_{n+\frac{1}{2}} \\ \underset{\sim}{H}_{n+1} \end{Bmatrix} \tag{34}$$

(33) takes a more convenient form,

$$(\bar{\underset{\sim}{M}}_1 + \theta\bar{\underset{\sim}{C}} + \bar{\underset{\sim}{D}})\, \underset{\sim}{X}_{n+1} = (\bar{\underset{\sim}{M}}_2 + (1-\theta)\bar{\underset{\sim}{C}} + \underset{\sim}{D}^T)\, \underset{\sim}{X}_n \tag{35}$$

Expressing $\underset{\sim}{X}_{n+1}$ as

$$\underset{\sim}{X}_{n+1} = \lambda \underset{\sim}{X}_n \tag{36}$$

and substituting (36) in (35) leads to

$$\lambda = \frac{m + \Delta t[(1-\theta)(-e) + d_s] - i\Delta t[d_{ss} + (1-\theta)c_{ss}]}{m + \Delta t[\theta(e) + d_s] = i\Delta t[d_{ss} + \theta c_{ss}]} \tag{37}$$

where $i = \sqrt{-1}$; $m>0$; $e>0$; subscript s signifies that the value stems from the symmetric part of the matrix; and ss denotes the skew symmetric contribution.

For $\theta = 0$, we obtain

$$\lambda = \frac{m + \Delta t d_s - \Delta t e - i\Delta t[d_{ss} + c_{ss}]}{m + \Delta t d_s + i\Delta t d_{ss}} \tag{38}$$

When eddy viscosity and Coriolis terms are neglected, (38) reduced to

$$|\lambda| = \left| \frac{m + \Delta t d_s - i\Delta t d_{ss}}{m + \Delta t d_s + i\Delta t d_{ss}} \right| = 1 \tag{39}$$

Therefore, under the given assumptions, the $\theta = 0$ split-time scheme is unconditionally stable. However, application of the method has revealed that instability sets in at Courant numbers larger than approximately 1.5. An explanation is not yet known, but possible sources of instability are non-linear effects, boundary conditions and bottom variation. This is obviously an area where more research is needed.

RESULTS. VERIFICATION STUDIES

The most desirable verification of a numerical model is a comparison with an "exact" analytical solution of the same system of equations. Fortunely, the analytical solution of standing waves in a 2-layered infinitely wide channel of length is known and we use this as a basis for verification. Figure 5 shows a side view of the channel and plans of two grid configurations.

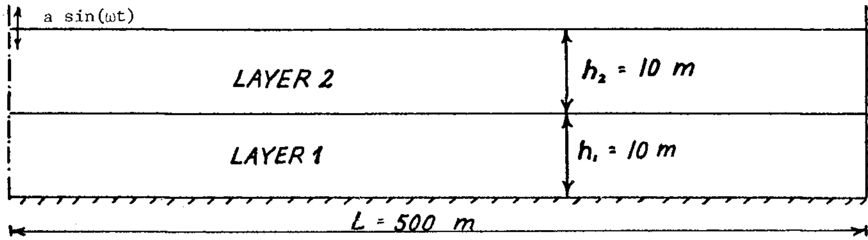

Side view of channel

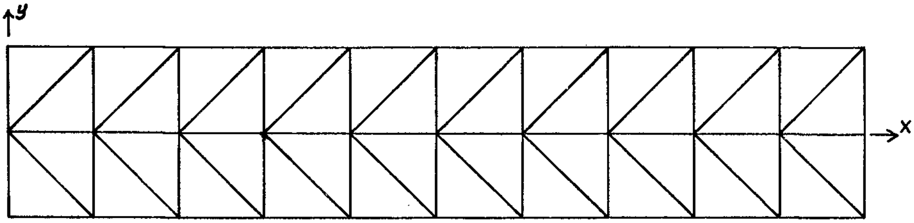

Plan view of channel with grid. Δx=50 m; Δy=50 m; Δt=2.5 sec.

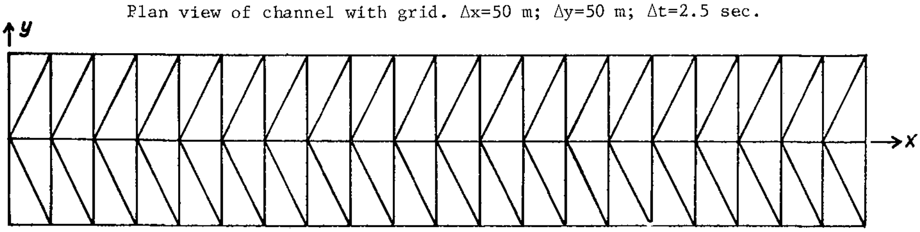

Plan view of channel with fine grid. Δx=25 m; Δy=50 m; Δt=1.25 sec.

Fig. 5. Sketch of first comparison study. Rectangular channel.

The solution for the surface and interface displacements η_1, η_2 with a forcing consisting of sinusoidal oscillation (amplitude a) of the surface and no movement of the interface at the entrance is given by

$$\eta_1 = \left\{ A\left(1 - \frac{gh_2}{\omega^2} k_1^2\right)\cos k_1 x + B\left(1 - \frac{gh_2}{\omega^2} k_2^2\right)\cos k_2 x \right\} \sin\omega t \tag{40}$$

$$\eta_2 = \left\{ A \cos k_1 x + B \cos k_2 x \right\} \sin\omega t \tag{41}$$

with

$$A = \frac{a\left(1 - \frac{gh_2}{\omega^2}k_2^2\right)}{(k_1^2 - k_2^2)\frac{gh_2}{\omega^2}\cos k_1 L}; \quad B = \frac{a\left(\frac{gh_1}{\omega^2}k_1^2 - 1\right)}{(k_1^2 - k_2^2)\frac{gh_2}{\omega^2}\cos k_2 L} \tag{42}$$

$$\begin{Bmatrix} k_1 \\ k_2 \end{Bmatrix} = \left[\frac{1}{2}\frac{\rho_1}{\Delta\rho}\frac{(h_1 + h_2)}{gh_1h_2}\omega^2 \pm \omega^2\sqrt{\left(\frac{1}{2}\frac{\rho_1}{\Delta\rho}\frac{(h_1 + h_2)}{gh_1h_2}\right)^2 - \frac{\rho_1}{\Delta\rho}\frac{1}{gh_1gh_2}}\,\right]^{\frac{1}{2}} \tag{43}$$

The numerical model was initialised with the correct values of elevations at maximum displacement (velocities zero) and then run with the forcing for several tidal periods ($T = 500$ sec).

The analytical results and absolute error in the numerical solution are plotted in figure 6. The agreement for the fine grid is reasonable although not impressive.

The forcing period T was increased to 1000 sec., so that the number of short waves in the channel is approximately 1. Results are plotted in figure 7 and show very good agreement. This indicated that about 20 points per full wave length are necessary with the linear element for an accurate representation.

The second comparison is only qualitative, since it is impossible to satisfy the same boundary conditions in analytical and numerical models. The problem involved determining of the harmonic oscillation in a rectangular basin with an opening on one side. The dimensions of the basin are chosen so as to approximate the Massachusetts Bay on the east coast of the U.S.

The analytical solution of this problem is developed in [3] and is expressed in terms of infinite Fourier series. Collocation was used to specify the boundary conditions as discussed in the reference. In the numerical computation, the free surface was subjected to a tidal excitation, and the interface surface was fixed at its initial position. A sample plot of layer velocities is shown in figure 8, which compares favorably with the analytical results in figure 9.

CONCLUSION

The value of a model is determined by its ability to describe actual physical processes. For this type of evaluation, much more data is needed. The finite element method appears advantageous with respect to flexible spatial discretization and treatment of boundary conditions. The formulation is independent of grid configuration and choice of element type, since the structure of the equations remains the same. Compared with well-known finite difference models, the bandwidth of the finite element coefficient matrix is usually larger but the finite element model requires less nodes, i.e., less unknowns. Thus storage requirements are usually somewhat less, but the finite element method might require more computations. Additional research needs to be done on the time integration in order to increase the time step. The ocean boundary conditions are extremely important and additional work is needed to determine those properly.

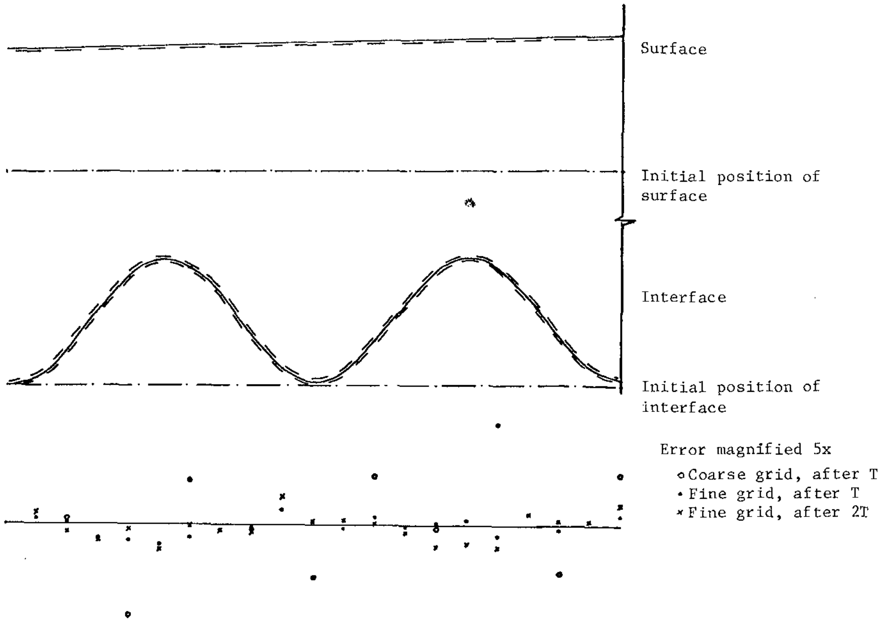

Fig 6. Comparison of solutions for rectangular channel. T=500sec.

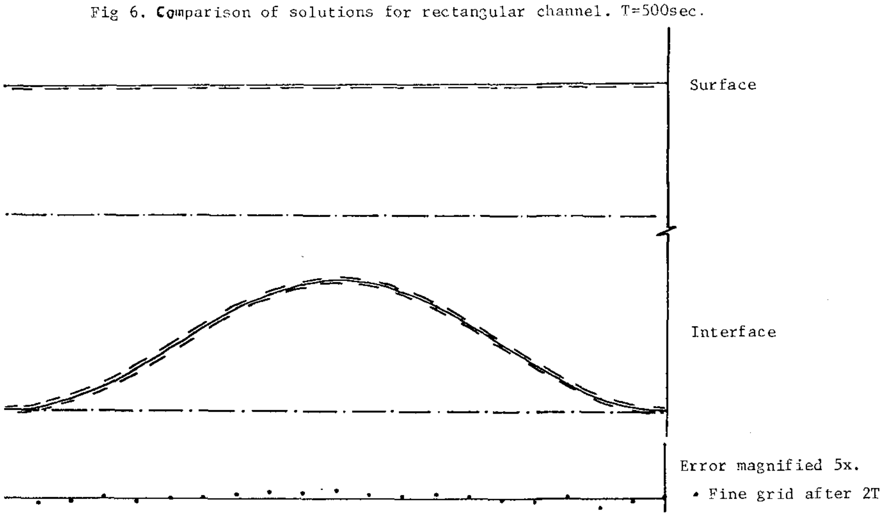

Fig. 7. Comparison of solutions for rectangular channel. T=1000 sec.

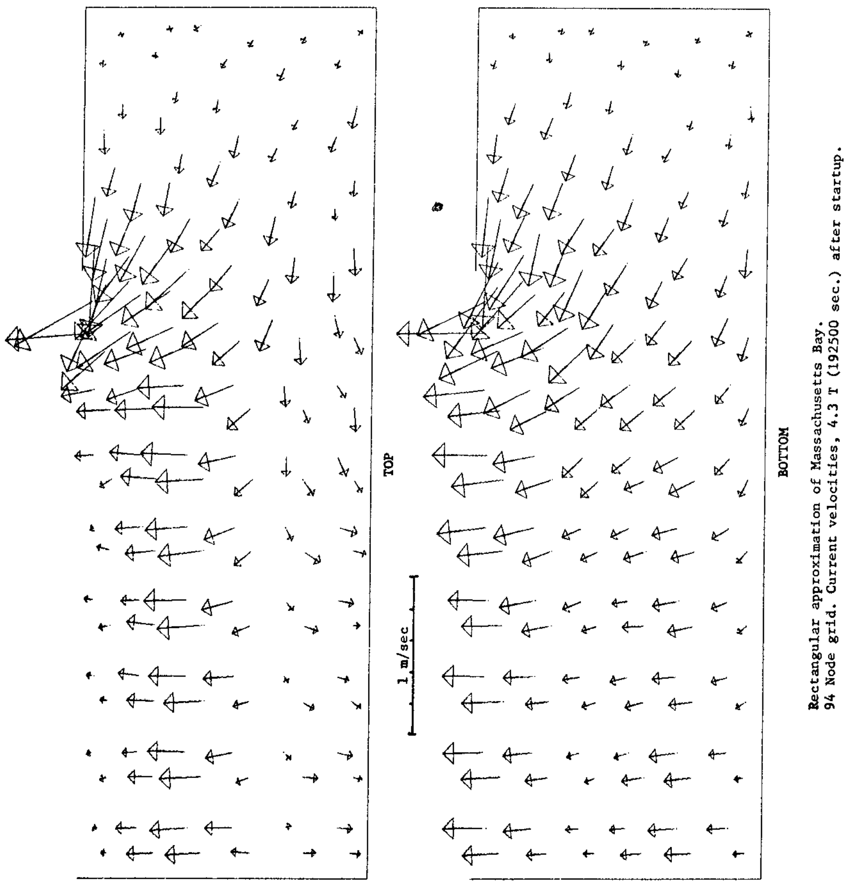

Fig. 8. Computed velocity field for two layered approximation of Massachusetts Bay.

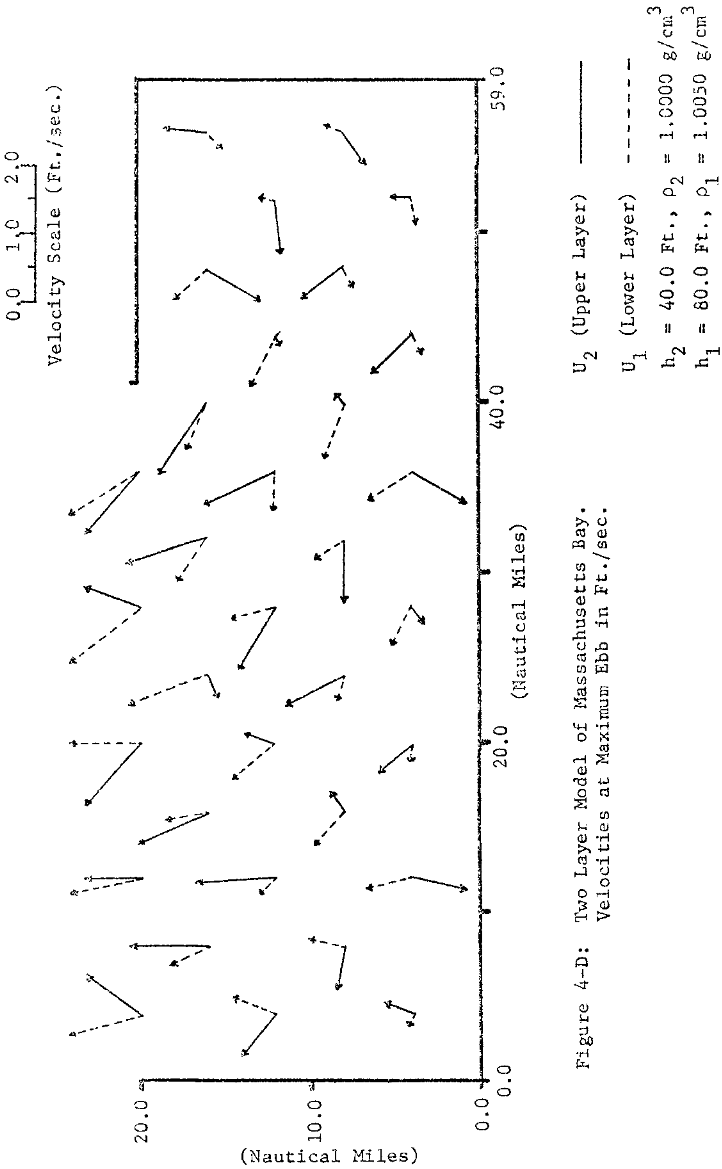

Fig. 9. Velocity field from analytical solution in ref. [3].

REFERENCES

1. Abbot, M.B., Gruber, J.P., "Towards a design system for stratified flows", Int. Symp. on Stratified Flows, IAHR, Novosibirsk, 1972.

2. Abraham, G., Eysink, W.D., "Magnitude of interfacial shear in exchange flow", J. Hydraulic Research, AlHR, Vol. 9, No.2, 1971.

3. Briggs, D.A., Madsen, O.S., "Analytical models for one- and two layer systems in rectangular basins", TR 172, part Il, R.M.Parsons Laboratory for Water Resources and Hydrodynamics, M.I.T., 1973.

4. Connor, J.J., Wang, J.D., "Finite element modeling of two-dimensional hydrodynamic circulation", TR 172, part 1, R.M.Parsons Laboratory for Water Resources and Hydrodynamics, M.I.T., 1973.

5. Csanady, G.T., "Turbulent diffusion in the environment", Geophysics and astrophysics monographs, D. Reidel Publishing Co., 1973.

6. Ladyzhenskaya, O.A., "The mathematical theory of viscous incompressible flow", Gordon and Breach, 2nd edition, 1969.

7. Leendertse, J.J., Alexander, R.C., Liu, L.-K., "A three-dimensional model for estuaries and coastal seas, Vol. I : Principles of computation, Rand Corp. 1973.

8. Loziuk, L.A., Anderson, U.C., Belytschko, T., "Transient hydrothermal analysis of small lakes", J. Power Division, ASCE, PO2, Nov. 1973.

9. Mikhlin, S.G., "Variational methods in mathematical physics", Pergamon Press, 1964,

10. Simons, T.J., "Development of three-dimensional numerical models of the great lakes", Canada Centre for Inland Waters, Scientific Report, 1971.

11. Starr, V.P., "Physics of negative viscosity", McGraw-Hill, 1968.

12. Strang, G., Fix, G.J., "An analysis of the finite element method", Prentice-Hall, 1973.

13. Wada, A., "Study of thermal diffusion in a two layer sea caused by outfall of cooling water", Int. Symp. on Stratified Flows, IAHR, Novosibirsk, 1972.